CrystEngComm

RSC Publishing

PAPER

View Article Online
View Journal | View Issue

Cite this: *CrystEngComm*, 2013, **15**, 4162

One-pot synthesis, formation mechanism and near-infrared fluorescent properties of hollow and porous α-mercury sulfide

Shikui Wu,*[ab] Chaojun Chen,*[a] Xiaoping Shen,*[b] Gang Li,[a] Lina Gao,[a] Amei Chen,[a] Jinfeng Hou[d] and Xingjie Liang[c]

Received 30th October 2012,
Accepted 16th March 2013

DOI: 10.1039/c3ce26777f

www.rsc.org/crystengcomm

Hollow and porous nanoparticles of α-mercury sulfide (cinnabar) have been synthesized with thioacetamide and mercury nitrate as precursors *via* a one-pot wet chemistry process. Scanning electron microscopy (SEM) and transmission electron microscopy (TEM) show the presence of plate-like hollow particles with uniform diameters of 70 ± 10 nm and thicknesses of 20 ± 5 nm. Moreover, the plate-like hollow particles have porous surfaces with a pore size of 6 ± 3 nm. High-resolution TEM images show highly ordered lattice fringes, indicating the high crystallinity of the plates and identifying the product to be made of α-HgS. A possible mechanism related to anion exchange accompanied by the Kirkendall effect is suggested. The band gaps and near-infrared fluorescent properties of the plate-like hollow and porous α-HgS particles were also investigated, indicating their potential applications as a fluorescent dye in biomedical fields.

Introduction

α-Mercury sulfide (α-HgS) as a vagarious material has been used as a semiconductor,[1] in optical applications,[2] and in medicine for the treatment of syphilis, psoriasis and other incurable diseases.[3–5] A criticism of the material is the potential toxicity and the lack of applications in biology, although some research proves that the adverse effects of α-mercury sulfide in traditional medicines seem to be tolerable and reversible at the therapeutic doses.[4] Despite the obvious perceived barrier for the use of mercury-containing nanomaterials, applications in biology are emerging in biomedical fields for applied and fundamental issues.[6–8] β-Mercury sulfide (β-HgS) as near-infrared quantum dots has also been noted by some teams,[9–11] because of its potential use in the optical imaging of live animals.[12] The present investigation attempts to use a simple wet-chemical and template-free method to prepare nanosized α-HgS for medicinal use. Interestingly, novel hollow and porous nanoparticles of α-HgS were obtained. Although α-HgS[13–17] and β-HgS[17–20] nanostructures with various morphologies have been prepared, to the best of our knowledge, this is the first report on hollow and porous α-HgS nanoplates.

Materials with hollow and/or porous nanostructures have larger specific surface areas compared to other solid morphologies, which makes them more applicable for catalysis, absorption and drug-delivery.[21–23] The infrared lattice bands of trigonal and cubic mercury sulfide have been reported by Riccius *et al.* in 1970s,[2] but the near-infrared (NIR)-emission of β-HgS nanostructures has been reported in recent years,[9–11] and the reports of α-HgS are limited.[2] In this study, the hollow porous structure and the near-infrared fluorescent properties of α-HgS nanoparticles are reported and demonstrated to have potential applications in near-infrared dyes, sensing, biomedical imaging and container functionality.[24] The possible anion exchange mechanism accompanied by the Kirkendall effect is suggested for the formation of the plate-like hollow and porous α-HgS nanoparticles.[25]

Materials and methods

Materials

The mercury(II) nitrate, thioacetamide, and nitric acid solvents used were purchased from Alfa Aesar Chemicals and used without further purification.

Synthesis of porous α-HgS nanoplates

In brief, 50 mL of mercury nitrate aqueous solution (0.125 g mercury nitrate) including 0.3 mL of concentrated nitric acid

[a]*School of Pharmacy, Inner Mongolia Medical University, Hohhot, 010059, P. R. China. E-mail: shikuiwu@yahoo.com; chenchaojun@163.com; Fax: +86 0471 665 3172; Tel: +86 0471 665 3172*
[b]*School of Chemistry and Chemical Engineering, Jiangsu University, Zhenjiang, 212013, P. R. China. E-mail: xiaopingshen@163.com*
[c]*CAS Key Laboratory for Biomedical Effects of Nanomaterials and Nanosafety, National Center for Nanoscience and Technology, Beijing, 100190, P. R. China*
[d]*Testing and Analysis Center, Inner Mongolia University of Technology, Hohhot, 010059, P. R. China*

(16 mol L^{-1}), and 50 mL of thioacetamide aqueous solution (0.375 g thioacetamide) were both added to a 150 mL three-neck flask under vigorous stirring. The resulting solution was heated up to 100 °C at a heating rate of 5 °C min^{-1}. The color of the solution changed from yellow to black and then to red. After 30 minutes, the sample was separated by centrifugation, and washed with water and ethanol 3 times. Then the red powder was heated at 110 °C for 24 hours. Powdered product was obtained.

Characterization of porous α-HgS nanoplate

The phases of the as-prepared products were characterized using powder X-ray diffraction (XRD, Rigaku D/MAX 2400) with Cu Kα radiation (λ = 1.5406 Å) at a scanning rate of 2° min^{-1}. The size, morphology and structure of the samples were characterized by field emission scanning electron microscopy (FESEM, Hitachi S-4800, with an accelerating voltage of 20 kV), selected area electron diffraction (ED), and high-resolution transmission electron microscopy (HRTEM, FET TECNAI F30, with an accelerating voltage of 200 kV). N_2 adsorption–desorption isotherms were obtained at 77 K on a Coulter SA 3100 surface area analyzer. The sample was pretreated for 12 h at 373 K under nitrogen before measurement. A UV-visible absorption spectrum of the colloid nanoplates dispersed in alcohol by sonication was recorded on a Shimadzu UV-2401PC UV-vis spectrophotometer. Room-temperature photoluminescence (PL) spectra were recorded on an RF-5301PC spectrometer with a 150 W Xenon lamp at an excitation wavelength of 473 nm. The fluorescence quantum yield (QY) of plate-like hollow and porous α-HgS nanoparticles was carefully measured according to references,[26] using cardiogreen as a fluorescence standard in DMSO with a QY of 13%.[27]

Results and discussion

Structural and morphological characterization

Fig. 1 shows the XRD pattern of the as-synthesized sample. All the diffraction peaks can be well indexed to the hexagonal phase HgS (cinnabar) (JCPDS, No. 6-0256). The calculated cell parameters are a = 4.174 Å and c = 9.483 Å. Moreover, no impurities are detected in the XRD pattern, suggesting the high purity of the product. It is noticeable that the (101) peaks are extremely strong compared with the standard reflections, which is probably related to the preferential growth of the hexagonal HgS nanoplates.[28] The products are proven to be well crystallized and pure by the XRD patterns.

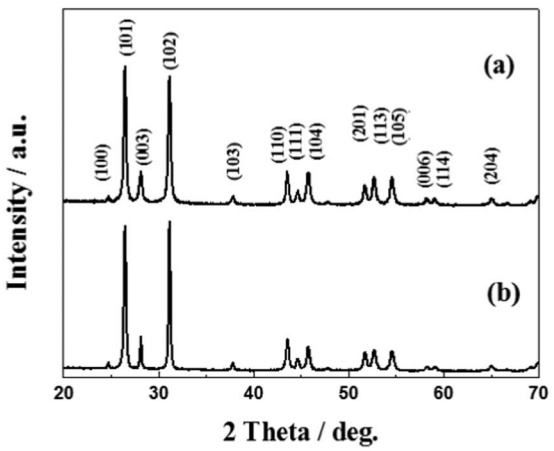

Fig. 1 Typical XRD patterns of the as-prepared product (a), and bulk α-HgS (b).

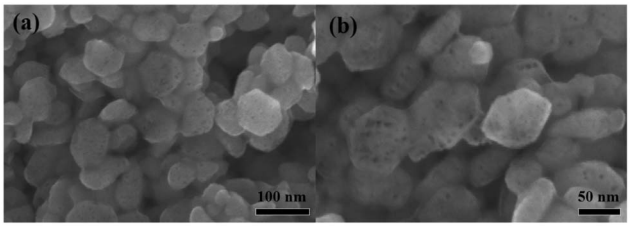

Fig. 2 FESEM images of the as-synthesized product at different magnifications.

The morphology of the as-synthesized products was investigated by FESEM. Fig. 2a shows a representative FESEM image of the product, which indicates that the product is composed of a large quantity of hexagon plate-like nanocrystals with diameters of 70 ± 10 nm and thicknesses of 20 ± 5 nm. From the high magnification FESEM image (Fig. 2b), it can be seen that the shapes of the hexagon nanoplates are regular with a large number of holes on their surfaces.

The novel nanostructure of the as-synthesized HgS nanoparticles was revealed by TEM. As shown in Fig. 3a, all the nanocrystals have porous plate-like shapes with an average pore size of 6 ± 3 nm. Fig. 3b shows the magnified side view of several nanoplates, and a strong contrast difference in all of the particles with a bright center surrounded by a much darker edge confirms their hollow architecture. The SAED pattern (inset in Fig. 3a) taken from a nanoplate lying on the HRTEM grid indicates that the nanoplates have a single-crystal structure. The HRTEM image (inset of Fig. 3b) reveals that the porous shells of the α-HgS plates are composed of some small crystallites (about 6 nm). Close inspection of the HRTEM images reveals that each crystalline domain extends from the outside surface to the inside of the shell, with a neighboring

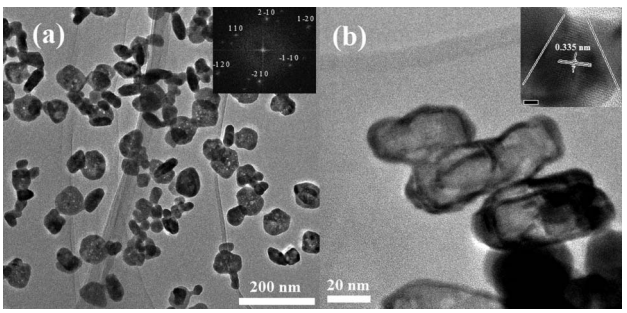

Fig. 3 TEM images of the as-synthesized product: (a) TEM images showing the porous plate-like shape; the inset is the corresponding selected-area electron diffraction (SAED) pattern; (b) high magnification TEM image showing the hollow structure, the inset is an HRTEM image.

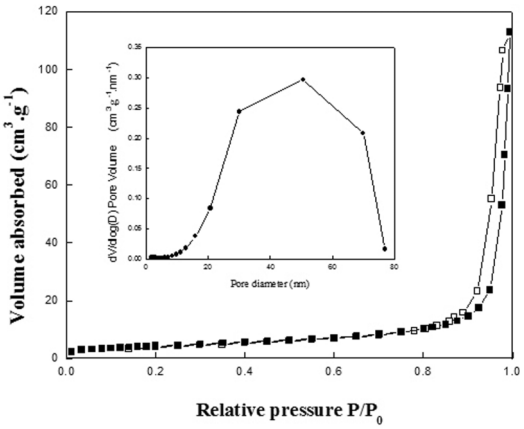

Fig. 4 N_2 adsorption–desorption isotherms and pore size distribution plot (inset) of the plate-like nano-HgS.

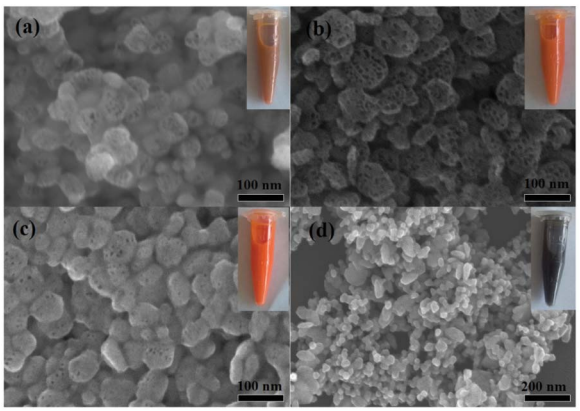

Fig. 5 The morphology and color (insets) of the HgS nanostructures tuned by the addition of different amounts of nitric acid: (a) 0.1 mL, (b) 0.2 mL, (c) 0.4 mL, (d) 0.5 mL.

crystal domain present on each side across a grain boundary. This implies that the plate-like particles are composed of some little single-crystals. The inter-planar distance was measured to be 0.335 nm, corresponding to the (101) plane of α-HgS. It is deduced that the growth of the nanoplates along the (101) direction would be hindered to make the (101) planes the basal planes of the nanoplates.

N_2 absorption and desorption analysis was used to further examine the porous structure, and the data is shown in Fig. 4. The isotherms feature type V curves with a hysteresis loop in the relatively high pressure range, which is related to the existence of mesopores. The specific surface area and pore volume are determined to be about 39.49 $m^2\ g^{-1}$ and 0.1749 $cm^3\ g^{-1}$, respectively. The average pore diameter of 50 nm and the broad pore size distribution of 3–79 nm (inset of Fig. 4) indicates mesoporous features. The isotherm of the α-HgS nanoplate sample exhibits a hysteresis loop in the p/p_0 range of 0.75–0.98 as shown in Fig. 4. This clearly indicates that the α-HgS nanoplate sample also exhibits a large textural porosity.[29,30] The BET analysis strongly supports the fact that the nanoplates have a mesoporous structure and more active sites present, which is attractive for drug-delivery applications.

Influence of nitric acid on the growth of α-HgS nanoplates

The starting pH value of the reaction mixture was adjusted using HNO_3 solution. The amount of nitric acid added is a crucial factor in the formation of HgS nanoplates. Fig. 5a shows the FESEM image of HgS nanoplates synthesized with the addition of 0.1 mL of 16 M nitric acid solution. The size of these particles was not uniform, and these particles did not transform to red α-HgS (inset of Fig. 5a). Red α-HgS can be obtained by adding 0.2–0.4 mL of HNO_3 solution. Hexagon disk-like particles start to form and are typically observed when 0.3 mL of nitric acid solution is added. The results are shown in Fig. 5b (0.2 mL), 2a (0.3 mL) and 5c (0.4 mL). But when the amount of nitric acid added was more than 0.5 mL, only black precipitate (a mixture of α-HgS and β-HgS) can be obtained, and the shape and size of the particles are irregular (Fig. 5d). The effect of nitric acid seems to relate to the speed of transformation of thioacetamide into H_2S. The detailed mechanism for the nanoplates is given below.

Possible formation mechanism of the hollow and porous α-HgS nanoplates

An understanding of how nanoparticles form is vital to developing better ways of controlling their morphology and size. A 'surface-protected etching' strategy, Ostwald ripening, the Kirkendall effect, and galvanic replacement have been used to explain the process of hollow and porous particle growth. Based on the results of TEM and XRD, we propose a formation mechanism for these HgS particles, which is composed of five stages, including nucleation, aggregation of the particle seeds, fusion, phase transition and Kirkendall ion exchange.[31,32] In this case, the formation of the α-HgS porous nanoplates may be a complex process. The possible formation process is shown in Scheme 1.

It is well known that thioacetamide can partly turn into H_2S slowly, in an HNO_3 solution.[33] The reaction of H_2S with Hg^{2+} can produce an HgS precipitate (Fig. 6a). After the initial nucleation of HgS, the very small particles grow into nanocrystals (Fig. 6b), and these nanocrystals have a tendency to aggregate. When heated, lots of new nanoparticles form to minimize the surface energy *via* a simple self-assembly process

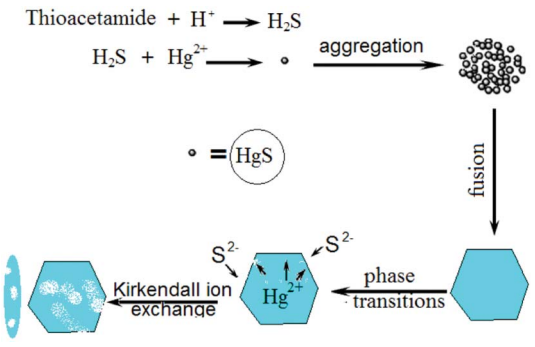

Scheme 1 Possible formation mechanism of the porous nanoplates.

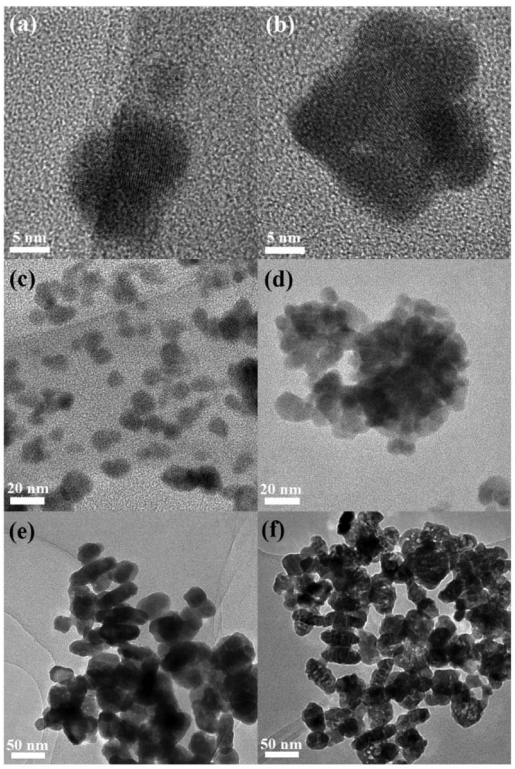

Fig. 6 TEM images of the nanoparticles synthesized with different reaction times: (a) 5 min, (b) 10 min, (c) 15 min, (d) 20 min, (e) 25 min, and (f) 30 min.

(Fig. 6c). It is believed that the solid spheres are composed of a large number of small nanoparticles (Fig. 6d). During the growth, owing to the difference in the surface energy, crystallites located in the inner of the solid plates (Fig. 6e) can be dissolved and merged by particles in the outer surface, meanwhile inward ion (S^{2-}) diffusion is limited and core species (Hg^{2+}) diffuse outward, generating a void space inside the nanoparticle (Fig. 6f). This is why the plates become bigger as the reaction time is increased.

UV-vis absorption and near-infrared fluorescent properties

The optical performances of semiconducting materials are critically dependent on their morphology and size.[34] Fig. 7 shows the UV-vis absorption and room-temperature photoluminescence (PL) spectra of the α-HgS porous plates. The UV-visible spectrum of the product is given in Fig. 7a. The material was dispersed in alcohol and then was sonicated for five minutes and the resulting solution was used to measure the absorption spectrum. A broad absorption peak with a maximum at around 370 nm is observed. This optical spectrum was used to calculate the band gap from

$$\alpha(\nu) = A(h\nu/2 - 2E_g)^{m/2} \quad (1)$$

where α is the absorption coefficient and E_g is the band gap. For a direct transition $m = 1$, a plot of $(\alpha E_{phot})^2$ *vs.* E_{phot} was constructed and the value of E_{phot} extrapolated to $\alpha = 0$ gave the band gap E_g.[35] The band gap calculated for the sample was 2.90 eV, which is higher than the band gap of bulk α-HgS (2.0 eV).[36]

The room-temperature PL spectrum displays a near-infrared fluorescence emission[37] band centered at 711 nm (with excitation wavelength 473 nm), as shown in Fig. 7b. The PL quantum yield of the obtained α-HgS nanoplates was 1.0%, which is attributed to type-II nanocrystal quantum dots.[9] The novel materials have far-reaching potential for the study of intracellular process at the single-molecule level, high resolution cellular imaging, long-term *in vivo* observation of cell trafficking, tumor targeting, and diagnostics.[38,39] Further work is under way.

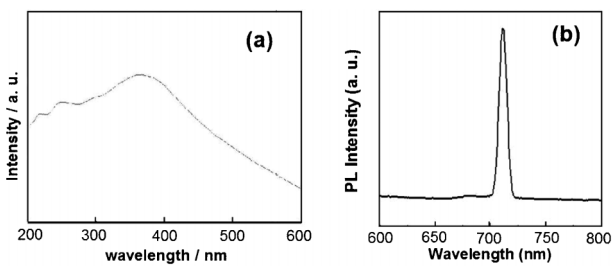

Fig. 7 (a) UV-visible absorption spectrum and (b) near-infrared fluorescence properties of hollow and porous α-HgS nanoplates.

Conclusions

In summary, hollow and porous α-HgS nanoplates were synthesized through a facile one-pot wet-chemical strategy. The UV-visible absorption and room-temperature photoluminescence spectra of the as-obtained hollow and porous α-HgS nanoparticles exhibited near-infrared fluorescent emission luminescence, indicating the quantum confinement effect. We hope that this simple method is general and can be applied to the synthesis of porous structures of any other semiconductors.

Acknowledgements

This work was supported by the Natural Science Foundation of Inner Mongolia (Grant No. 2012MS1209), National Natural Science Foundation of China (Grant No. 81260650), and the Young Foundation of Inner Mongolia Medical University.

References

1 R. S. Davidson and C. J. Willsher, *Nature*, 1979, **21**, 238.
2 H. D. Riccius and K. J. Siemsen, *J. Chem. Phys.*, 1970, **52**, 4090.
3 J. Liu, J. Shi and L. Yu, *Exp. Biol. Med.*, 2008, **233**, 810.
4 P. Padhi, G. Sahoo and S. Panigrahi, *AIP Conf. Proc.*, 2008, **1063**, 431.
5 T. Efferth, P. Li and B. Kaina, *Trends Mol. Med.*, 2007, **13**, 353.
6 F. Mei, X. He, W. Li and Y. Zhang, *J. Fluoresc.*, 2008, **18**, 883.

7 S. Rath, G. Chainy and S. Nozaki, et al., *Phys. E.*, 2005, **30**, 182.
8 N. Morgan, S. English and W. Chen, et al., *Acad. Radiol.*, 2005, **12**, 313.
9 J. Yang, W. Zhang, Y. Hu and J. Yu, *J. Colloid Interface Sci.*, 2012, **379**, 8.
10 W. Wichiansee, M. N. Nordin, M. Green and R. J. Curry, *J. Mater. Chem.*, 2011, **21**, 7331.
11 K. A. Higginson, M. Kuno, J. Bonevich, S. B. Qadri, M. Yousuf and H. Mattoussi, *J. Phys. Chem. B*, 2002, **106**, 9982.
12 A. Smith, M. Mancini and S. Nie, *Nat. Nanotechnol.*, 2009, **4**, 710.
13 A. K. Mahapatra and A. K. Dash, *Phys. E.*, 2006, **35**, 9.
14 F. Oshal and H. Mossalayi, *Pharma Chem.*, 2010, **2**, 33.
15 X. Chen, X. Wang, Z. Wang, X. Yang and Y. Qian, *Cryst. Growth Des.*, 2005, **5**, 347.
16 T. Ren, S. Xu, W. Zhao and J. Zhu, *J. Photochem. Photobiol., A*, 2005, **173**, 93.
17 H. Wang and J. Zhu, *Ultrason. Sonochem.*, 2004, **11**, 293.
18 L. Wu, B. Quan and Y. Liu, *ACS Nano*, 2011, **5**, 2224.
19 P. G. Sheikhiabadi, F. Davar and M. Salavati-Niasari, *Inorg. Chim. Acta*, 2011, **376**, 271.
20 J. Lv, Y. Feng, S. Zhang and J. Guo, *Mater. Lett.*, 2005, **59**, 3109.
21 J. Zheng, X. Wang and W. Li, *CrystEngComm*, 2012, **14**, 7616.
22 H. Goesmann and C. Feldmann, *Angew. Chem., Int. Ed.*, 2010, **49**, 1362.
23 G. Dong and Y. Zhu, *CrystEngComm*, 2012, **14**, 1805.
24 X. Michalet, F. F. Pinaud and S. Weiss, *Science*, 2005, **307**, 538.
25 J. Park, H. Zheng and A. P. Alivisatos, *J. Am. Chem. Soc.*, 2009, **131**, 13943.
26 M. Grabolle, M. Spieles, V. Lesnyak, N. Gaponik, A. Eychmuller and U. Resch-Genger, *Anal. Chem.*, 2009, **81**, 6285.
27 R. C. Benson and H. A. Kues, *J. Chem. Eng. Data*, 1977, **22**, 379.
28 X. Chen, X. Wang and Z. Wang, *Cryst. Growth Des.*, 2005, **5**, 347.
29 Y. Jia, X. Yu and T. Luo, *Dalton Trans.*, 2013, **42**, 1921.
30 J. Huang, X. Xu and C. Gu, *Mater. Res. Bull.*, 2012, **47**, 3224.
31 S. Chen, X. Zhang and W. Tan, *Cryst. Growth Des.*, 2010, **10**, 1257.
32 S. Zhong, R. Xu and A. Xu, *J. Mater. Chem.*, 2011, **21**, 16574.
33 T. Nomura, Y. Kousaka, M. Alonso and M. Fukunaga, *J. Colloid Interface Sci.*, 2000, **223**, 179.
34 W. Wichiansee, M. N. Nordin and R. J. Curry, *J. Mater. Chem.*, 2011, **21**, 7331.
35 P. S. Nair, T. Radhakrishnan and P. O'Brien, *J. Mater. Chem.*, 2004, **14**, 581.
36 W. Taylor, A. Pinczuk and E. Burstein, *Phys. Rev. B: Solid State*, 1970, **1**, 4058.
37 R. Weissleder and V. Ntziachristos, *Nat. Med.*, 2003, **9**, 123.
38 S. Kim, B. Fisher and M. Bawendi, *J. Am. Chem. Soc.*, 2003, **125**, 11466.
39 S. Kim, Y. T. Lim and J. Lee, *Nat. Biotechnol.*, 2004, **22**, 93.

